Aerodynamic Model Identification using the Two-Step Approach

Federico Paredes Vallés*

System Identification of Aerospace Vehicles (AE4320), Delft University of Technology

This report is concerned with the implementation of the Two-Step Identification Approach to a set of flight-test data in order to estimate the aerodynamic model of the Cessna Citation II aircraft. In order to do so, the well-known extended Kalman filter (EKF) is used for the flight path reconstruction problem and its results present a remarkable level of accuracy. Once the flight path trajectory has been reconstructed, the aerodynamic model becomes linear-in-the-parameters, so the Ordinary Least Squares (OLS) regression method is implemented and applied to estimate these aerodynamic coefficients. Apart from the estimation, this report also presents the validation of these coefficients by means of a model residual analysis in order to ensure the level of accuracy. Finally, this section analyzes which parameters are dominant and which have the least influence in the data fitting of this identification step. Furthermore, it demonstrates that the fact of augmenting the aerodynamic model with extra parameters does not improve the quality of the estimation.

I. Introduction

The term system identification can be understood as the process of developing or improving a mathematical representation of a physical system based on observed data. As stated in [1], its application consists of three different steps: system modeling, which implies modeling a dynamical system from first principles via physical laws; test specification and execution in order to store experimental data using sensors; and parameter identification using optimization procedures.

The fact of representing a system by means of a mathematical model is an essential advantage in any engineering field, both for research and industrial activities, especially for those related with the development of control systems and simulators in the aerospace field. On one hand, system identification techniques play a crucial role for model based control design, where the performance of the controllers is directly related with the similarity between the model and the aircraft in real flight. For flight control purposes, increasingly popular nonlinear control strategies as Nonlinear Dynamic Inversion (NDI) and Incremental Nonlinear Dynamic Inversion (INDI) are clear examples that the need for accurate nonlinear aerodynamic models has grown [2]. On the other hand, flight simulators are increasingly used not only for pilot training, but also for other applications such as flight planning, envelope expansion, design and analysis of control laws, handling qualities investigations, pilot-in-the-loop studies, and to reduce flight-test time, cost, and risks [3,4]. These applications demand advanced models and high-fidelity aerodynamic databases of flight vehicles that are generated using system identification techniques from flight data. Apart from these two major applications, the interest in obtaining accurate vehicle model characteristics also comes from the desire to better understand theoretical predictions of physical phenomena and to validate wind-tunnel test results.

*Federico Paredes Vallés (4439953) is with the Department of Control and Simulation of the Faculty of Aerospace Engineering, Delft University of Technology. Email: F.ParedesValles@student.tudelft.nl.

One of the most successful techniques applied to system identification in the aerospace field is the well-known "Two-Step Approach". It basically consists in splitting the identification problem into two distinct parts: state estimation and parameter identification. The state estimation part, also named as flight path reconstruction (FPR) [5] or compatibility check [6], is based on the validation and correction of flight test data by means of using measurements and mathematical models of the system under analysis. In other words, this reconstruction problem means the estimation of the unknown parameters –states– of the aircraft kinematic model during a specific maneuver. The importance of this first estimation step relies on the fact that real sensors present biases that must be accounted for in the subsequent phases of the analysis. Once the flight path trajectory has been reconstructed, the aerodynamic model becomes linear-in-the-parameters, so simple regression methods can then be applied to estimate these dynamic coefficients. This is considered to be a great advantage of the Two-Step Approach, which can be implemented recursively and therefore, it is suitable for real-time applications [1].

In order to accomplish the FPR step, output-error and filter-error methods have been used for state estimation [7]. Whereas the former approach can handle only measurement errors [8], the latter is also able to deal with process noise in addition to measurement noise [9]. Among the filter-error methods, the Extended Kalman Filter (EKF) and its iterated version (IEKF) are the most commonly used algorithms, and the ones treated in this report, while the Unscented Kalman Filter (UKF) is becoming popular because of its competitive computational cost [10,11].

An alternative to the Two-Step Approach is the "Maximum Likelihood method" which attempts to solve the joint state and parameter estimation problem by searching for the global optimum of a likelihood function composed of output errors or prediction errors. This method is based on the idea that a good estimate of an unknown parameter would be the value that maximizes the probability –likelihood– of getting the observed data. In [12], Dr.ir. Chu et al pointed out that better results can be obtained through the maximum likelihood method, however, convergence problems may often be encountered when applying this approach to a large number of unknown parameters.

A more recent approach to modeling nonlinear dynamical systems is the use of artificial neural networks (ANN). In machine learning, these networks can be regarded as a functional imitation of biological neural networks and as such they share some advantages that biological organisms have over standard computational systems [13]. These networks are essentially black-box models that use global basis functions in order to estimate or approximate any nonlinear function to an arbitrarily high degree of accuracy from a limited amount of training data [14]. The adjustment of the ANN parameters results in different shaped nonlinearities achieved through a gradient descent approach on an error function –error backpropagation– that measures the difference between the output of the network and the output of the true system for given input data or input-output data pairs [15]. Although neural networks are powerful function approximators and a useful approach when identifying a physical process, as stated in [16], they suffer from numerical instabilities and are inherently intransparent as a result of their black-box nature.

Although it has not been pointed out yet in the report, the current consensus in aerodynamic model identification is to assume a polynomial model structure for each of the aerodynamic coefficients, after which estimation techniques are employed to estimate the parameters such that they, in some way, optimally fit a set of data. As stated by Dr.ir. de Visser in [17], the limited approximation power of polynomials requires the design of flight test maneuvers specifically designed to reduce the effects of dimensional couplings and high order nonlinearities such that the resulting datasets can be adequately modeled. Recently, the multivariate simplex B-spline was presented as an alternative for fitting the flight data of more complex maneuvers that cover a larger region of the flight envelope [16]. The main benefit of this technique over neural networks is the fact that it is linear in the parameters, which allows for the use of efficient least squares solvers. Furthermore, the great promise of the multiplex spline lies in the fact that variables can be decoupled within a single spline model. This implies that there is more freedom to incorporate knowledge of the system in the model structure [18].

Despite these advanced system identification techniques, this report illustrates the development and application of the Two-Step approach to a real-life flight test dataset obtained with the Cessna Citation II laboratory aircraft owned by Delft University of Technology. Additionally, a least squares parameter estimator is derived for estimating the parameters of a linear aerodynamic model structure.

This report is organized as follows. First of all, the nonlinear mathematical models that describe the kinematic equations and the observation model of the aircraft are introduced in Section II. This first step is of crucial importance because it is where the design of the integrated GPS/IMU/Airdata navigation system

takes place. Section III presents the implementation and application of the Extended Kalman Filter to the aforementioned navigation system; the estimation of all aircraft states together with accelerometer/gyro unknown parameters and wind components; and a proof of convergence of the algorithm. Then, Section IV consists of the required steps to proceed with the identification of the aerodynamic model of the aircraft via least-squares algorithms. Finally, concluding remarks are present.

II. Aircraft kinematic and observation models

This section presents the mathematical models that will be used in the flight path reconstruction (FPR) task that is subsequently explained in Section III. These models can be classified as kinematic models and observation models. On one hand, kinematic models are a special form of the equations of motion of an aircraft in which specific aerodynamic forces $\{A_x, A_y, A_z\}$ and angular rates $\{p, q, r\}$ serve as input, as presented in Eq. (1).

$$\underline{\boldsymbol{u}} = col(A_x, A_y, A_z, p, q, r) \tag{1}$$

Kinematic model

Aircraft equations of motion take the form of three sets of first-order differential equations as presented in [19]. First of all, the position of the aircraft's center of gravity relative to the earth-fixed reference frame –also known as navigation reference frame F_n– is computed by numerically integrating the following set of equations.

$$\begin{bmatrix} \dot{x}_n \\ \dot{y}_n \\ \dot{z}_n \end{bmatrix} = L_{EB} \begin{bmatrix} u_b \\ v_b \\ w_b \end{bmatrix} + \begin{bmatrix} W_{x_n} \\ W_{y_n} \\ W_{z_n} \end{bmatrix}$$

$$L_{EB} = \begin{bmatrix} \cos(\theta)\cos(\psi) & \sin(\phi)\sin(\theta)\cos(\psi) - \cos(\phi)\sin(\psi) & \cos(\phi)\sin(\theta)\cos(\psi) + \sin(\phi)\sin(\psi) \\ \cos(\theta)\sin(\psi) & \sin(\phi)\sin(\theta)\sin(\psi) + \cos(\phi)\cos(\psi) & \cos(\phi)\sin(\theta)\sin(\psi) - \sin(\phi)\cos(\psi) \\ -\sin(\theta) & \sin(\phi)\cos(\theta) & \cos(\phi)\cos(\theta) \end{bmatrix} \tag{2}$$

In Eq. (2), the parameters $\{W_{x_n}, W_{y_n}, W_{z_n}\}$ denote the components of a unknown constant atmospheric wind vector W_n along the axes of F_n, which needs to be estimated in the flight reconstruction part of the Two Step Approach. Note that these wind components can be considered constant because of the relatively short flight tests that correspond to the datasets that are being used in the simulations presented in this report. This assumption is no longer valid in cases of long flight paths.

The second set of differential equations relates the first-order derivatives of the aircraft's velocities in the body-fixed reference frame F_b with the aforementioned specific aerodynamic forces, attitude angles, and angular rates.

$$\begin{aligned} \dot{u}_b &= (A_{x_m} - \lambda_x - w_x) - g\,\sin(\theta) - (q_m - \lambda_q - w_q)\,w_b + (r_m - \lambda_r - w_r)\,v_b \\ \dot{v}_b &= (A_{y_m} - \lambda_y - w_y) + g\,\cos(\theta)\sin(\phi) - (r_m - \lambda_r - w_r)\,u_b + (p_m - \lambda_p - w_p)\,w_b \\ \dot{w}_b &= (A_{z_m} - \lambda_z - w_z) + g\,\cos(\theta)\cos(\phi) - (p_m - \lambda_p - w_p)\,v_b + (q_m - \lambda_q - w_q)\,u_b \end{aligned} \tag{3}$$

Finally, the orientation of F_b with respect to F_n is governed by a third set of first-order differential equations for the Euler angles:

$$\begin{aligned} \dot{\phi} &= (p_m - \lambda_p - w_p) + (q_m - \lambda_q - w_q)\,\sin(\phi)\tan(\theta) + (r_m - \lambda_r - w_r)\,\cos(\phi)\tan(\theta) \\ \dot{\theta} &= (q_m - \lambda_q - w_q)\,\cos(\phi) - (r_m - \lambda_r - w_r)\,\sin(\phi) \\ \dot{\psi} &= (q_m - \lambda_q - w_q)\,\sin(\phi)\sec(\theta) + (r_m - \lambda_r - w_r)\,\cos(\phi)\sec(\theta) \end{aligned} \tag{4}$$

Eqs. (2), (3), and (4) represent the kinematic model for the motion –position, speed, and attitude– of the body-fixed reference frame of the aircraft attached to its center of gravity, with respect to a flat and non-rotating earth.

As it is possible to infer from Eqs. (3) and (4), the components of the input vector of $\underline{\boldsymbol{u}}$ are not used in these expressions. The reason for this relies in the fact that the measurements included in the input vector –specific aerodynamic forces and angular rates– are obtained using an on-board Inertial Measurement Unit (IMU) with its corresponding sensor biases, $\underline{\boldsymbol{\lambda}}$, and process noise, $\underline{\boldsymbol{w}}$, modifying the original input signal in $\underline{\boldsymbol{u}}$. Based on this, the realistic input vector that is used in the FPR task is described in Eq. (6).

$$\begin{array}{rl} A_{x_m} &= A_x + \lambda_x + w_x \\ A_{y_m} &= A_y + \lambda_y + w_y \\ A_{z_m} &= A_z + \lambda_z + w_z \\ p_m &= p + \lambda_p + w_p \\ q_m &= q + \lambda_q + w_q \\ r_m &= r + \lambda_r + w_r \end{array} \quad \rightarrow \quad \begin{array}{rl} A_x &= A_{x_m} - \lambda_x - w_x \\ A_y &= A_{y_m} - \lambda_y - w_y \\ A_z &= A_{z_m} - \lambda_z - w_z \\ p &= p_m - \lambda_p - w_p \\ q &= q_m - \lambda_q - w_q \\ r &= r_m - \lambda_r - w_r \end{array} \tag{5}$$

$$\underline{\boldsymbol{u_m}} = col(A_{x_m}, A_{y_m}, A_{z_m}, p_m, q_m, r_m) \tag{6}$$

Note that the real biases of the accelerometers and rate gyros included in the IMU are unknown, constant, and need to be estimated in the first step of the Two Step Identification Approach. Furthermore, the process noise $\underline{\boldsymbol{w}}$ is assumed to be white Gaussian noise with zero mean and a covariance matrix Q as now presented.

$$Q = diag(\sigma^2_{w_x}, \sigma^2_{w_y}, \sigma^2_{w_z}, \sigma^2_{w_p}, \sigma^2_{w_q}, \sigma^2_{w_x r}) \quad \text{with} \quad \begin{bmatrix} \sigma_{w_x} = 0.001\ m/s^2; & \sigma_{w_p} = 1.7453 \cdot 10^{-5}\ rad/s; \\ \sigma_{w_y} = 0.001\ m/s^2; & \sigma_{w_q} = 1.7453 \cdot 10^{-5}\ rad/s; \\ \sigma_{w_z} = 0.001\ m/s^2; & \sigma_{w_r} = 1.7453 \cdot 10^{-5}\ rad/s; \end{bmatrix} \tag{7}$$

Based on these unknown parameters – wind components and sensor biases – the state vector that consisted of position, velocities, and attitude components is augmented to include these additional unknowns, as introduced in Eq. (7):

$$\underline{\boldsymbol{x}} = col(x, y, z, u_b, v_b, w_b, \phi, \theta, \psi, \lambda_x, \lambda_y, \lambda_z, \lambda_p, \lambda_q, \lambda_r, W_{x_n}, W_{y_n}, W_{z_n}) \tag{8}$$

Observation model

On the other hand, the observation model describes the nonlinear algebraic relations among certain measured variables, such as airspeed and the position of the aircraft, to the components of the state and input vector as defined in Eqs. (6) and (7). The flight path reconstruction problem presented in this report is based on an observation model that is derived from a GPS receiver, which is responsible of providing aircraft position, ground speed earth components and attitude; and airdata sensors, which will offer processed true airspeed, angle of attack, and side slip angle of the aircraft.

In order to properly estimate the state vector using the Two Step approach, the fact of understanding the relationships between these observed parameters with the states of the aircraft is of relevant importance. For the case of the GPS receiver, all the expressions that are required have already been introduced in this report. On one hand, the GPS position and attitude are directly linked with the position and attitude in the state vector, respectively. On the other hand, the GPS ground speed of the aircraft is defined by means of using the right hand side of Eq. (2). For the case of airdata sensors, these variables are defined based on several components of the state vector, as now presented:

$$V = \sqrt{u_b^2 + v_b^2 + w_b^2}; \qquad \alpha = \tan^{-1}\left(\frac{w_b}{u_b}\right); \qquad \beta = \tan^{-1}\left(\frac{v_b}{\sqrt{u_b^2 + w_b^2}}\right); \tag{9}$$

As in the case of the IMU, the GPS receiver and airdata sensors are also affected by noise, known as the measurement noise $\underline{\boldsymbol{v}}$ in this case, which is assumed to be white Gaussian noise uncorrelated with the process noise, with zero mean and a covariance matrix R given by:

$$R = diag(\sigma^2_{v_x}, \sigma^2_{v_y}, \sigma^2_{v_z}, \sigma^2_{v_{u_n}}, \sigma^2_{v_{v_n}}, \sigma^2_{v_{w_n}}, \sigma^2_{v_\phi}, \sigma^2_{v_\theta}, \sigma^2_{v_\psi}, \sigma^2_{v_V}, \sigma^2_{v_\alpha}, \sigma^2_{v_\beta}) \quad \text{with}$$

$$\begin{bmatrix} \sigma_{v_x} = 10\ m; & \sigma_{v_{u_n}} = 0.1\ m/s; & \sigma_{v_\phi} = 1.7453 \cdot 10^{-3}\ rad/s; & \sigma_{v_V} = 0.1\ m/s; \\ \sigma_{v_y} = 10\ m; & \sigma_{v_{v_n}} = 0.1\ m/s; & \sigma_{v_\theta} = 1.7453 \cdot 10^{-3}\ rad/s; & \sigma_{v_\alpha} = 1.7453 \cdot 10^{-3}\ rad/s; \\ \sigma_{v_z} = 10\ m; & \sigma_{v_{w_n}} = 0.1\ m/s; & \sigma_{v_\psi} = 1.7453 \cdot 10^{-3}\ rad/s; & \sigma_{v_\beta} = 1.7453 \cdot 10^{-3}\ rad/s; \end{bmatrix} \tag{10}$$

Based on this reasoning, the observation vector is defined as:

$$\underline{\boldsymbol{z}}_{\boldsymbol{m}} = col(x_m, y_m, z_m, u_{b_m}, v_{b_m}, w_{b_m}, \phi_m, \theta_m, \psi_m, V_m, \alpha_m, \beta_m) \tag{11}$$

Once these two models have been described, it is possible to introduce the complete model that will be used in Section III during the flight path reconstruction task of the Two Step Approach. This model is now presented:

$$\begin{aligned} \dot{\underline{\boldsymbol{x}}}(t) &= \underline{\boldsymbol{f}}\left[\underline{\boldsymbol{x}}(t), \underline{\boldsymbol{u}}_{\boldsymbol{m}}(t), t\right] + \boldsymbol{G}\left[\underline{\boldsymbol{x}}(t)\right]\underline{\boldsymbol{w}}(t), \qquad \underline{\boldsymbol{x}}(t_0) = \underline{\boldsymbol{x}}_{\boldsymbol{0}} \\ \underline{\boldsymbol{z}}_{\boldsymbol{m}}(t_i) &= \underline{\boldsymbol{h}}\left[\underline{\boldsymbol{x}}(t_i), \underline{\boldsymbol{u}}_{\boldsymbol{m}}(t_i), t_i\right] + \underline{\boldsymbol{v}}(t_i), \qquad t = t_i, \quad i = 1, 2, ... \end{aligned} \tag{12}$$

where functions $\underline{\boldsymbol{f}}$ and $\underline{\boldsymbol{h}}$ are general nonlinear functions describing the kinematic and observation models respectively, and $\boldsymbol{G}$ is the system noise input matrix containing the parameters that multiply the process noise $\underline{\boldsymbol{w}}$. Regarding the noise vectors, these are defined as:

$$\begin{aligned} \underline{\boldsymbol{w}} &= col(w_x, w_y, w_z, w_p, w_q, w_r) \\ \underline{\boldsymbol{v}} &= col(v_x, v_y, v_z, v_u, v_v, v_w, v_\phi, v_\theta, v_\psi, v_V, v_\alpha, v_\beta) \end{aligned} \tag{13}$$

III. Flight Path Reconstruction

As previously mentioned in this report, the first step of the Two-Step Identification Approach consists in a nonlinear state reconstruction problem. This section presents the theory behind the Extended Kalman Filter (EKF) algorithm that has been used for this task, its implementation, and the results obtained.

III.A. Extended Kalman Filter

The Kalman filter is an estimation algorithm, rather than a filter [20]. This algorithm maintains real-time estimates of the states of the aircraft that are in continuous change. These estimates are updated using a stream of measurements – coming from the the integrated GPS/IMU/Airdata navigation system – that are subject to noise as previously introduced in Section II. As it is about to be explained in this section, the working principle of the Kalman filter is the calculation of a weighted average between the measured and the predicted state. To accomplish this goal, the Kalman filter uses knowledge of the deterministic and statistical properties of the aircraft states and measurements to obtain estimates given the information available. To enable semi-optimal weighting of the data, the Kalman filter algorithm maintains a set of uncertainties in its estimates and a measure of the correlations between the errors in the estimates of the different parameters.

III.A.1. Implementation of the EKF

For the state estimation problem introduced in the report, the true system state is not available and needs to be estimated in this first step of the Two-Step Approach. The initial state x_0 is assumed to follow a known Gaussian distribution with a covariance matrix denoted by P_0. The objective is to estimate the state at each time step by the process model and the observations that are available, although they are subjected to white noise as introduced before.

Based on Eq. (12), the nonlinear process model (from time k to time $k+1$), and the observation model at time $k+1$ are described in discrete time as:

$$\begin{aligned} \boldsymbol{x}_{k+1} &= \boldsymbol{f}(\boldsymbol{x}_k, \boldsymbol{u}_k) + \boldsymbol{G}(\boldsymbol{x}_k)\boldsymbol{w}_k \\ \boldsymbol{z}_{k+1} &= \boldsymbol{h}(\boldsymbol{x}_{k+1}) + \boldsymbol{v}_{k+1} \end{aligned} \tag{14}$$

The algorithm is based on the assumption that if the knowledge on the system state vector at time k can be expressed by means of a Gaussian distribution characterized by an average value $\overline{\boldsymbol{x}}_{k,k}$ and a covariance matrix $P_{k,k}$, in other words $\boldsymbol{x}_k \sim N\left(\overline{\boldsymbol{x}}_{k,k}, P_{k,k}\right)$; then the knowledge of $\boldsymbol{x}_{k+1}$ follows $\boldsymbol{x}_{k+1} \sim N\left(\overline{\boldsymbol{x}}_{k+1,k+1}, P_{k+1,k+1}\right)$. Then, the estimated value for the state vector $\boldsymbol{x}_{k+1,k+1}$ and the corresponding covariance matrix $P_{k+1,k+1}$ can obtained by means of using the Extended Kalman Filter. For a better understanding of the working principle of this algorithm, all the steps that need to be recursively applied are now presented with a brief explanation. A complete derivation of the EKF can be found in [20, 21].

Step 1: One-step ahead prediction

Since the original system state equation is nonlinear, the one-step ahead prediction can be calculated directly by integrating the nonlinear state equation with the earlier estimate of the state vector.

$$\underline{\hat{x}}_{k+1,k} = \underline{\hat{x}}_{k,k} + \int_{t_k}^{t_{k+1}} \underline{f}\left(\underline{\hat{x}}_{k,k}, \underline{u}_k^*, t\right) dt \tag{15}$$

where $\underline{\hat{x}}_{k+1,k}$ and $\underline{u}_k^*$ represent the nominal values that are used in order to linearize the nonlinear models in the incoming steps.

From Eq. (12), it is possible to infer that this prediction step can also be expressed as a set of ordinary differential equations. Therefore, it can be solved by means of using the `ode45` or Runge-Kutta algorithms in MATLAB, which notably eases the completion of this part.

Step 2: Calculate Jacobians

This step consists of the computation of the Jacobian matrices that correspond to the aircraft kinematic model and observation model when derived with respect to all the elements in the state vector, as presented in Eq. (8).

$$F_x(\cdot) = \frac{\partial}{\partial \underline{x}} f\left(\underline{x}(t), \underline{u}(t), t\right); \quad H_x(\cdot) = \frac{\partial}{\partial \underline{x}} h\left(\underline{x}(t), \underline{u}(t), t\right); \tag{16}$$

Step 3: Discretize the transition and input matrices

Once the Jacobian matrices have been computed, MATLAB allows to use the command `c2d` in order to convert the Jacobian of $\boldsymbol{f}$, $F_x(\cdot)$, and the system noise input matrix G from continuous to discrete time according to the formulas introduced in Eqs. (17) and (18).

$$\Phi_{k+1,k}(\cdot) = \exp\left[F_x(\cdot)(t_{k+1} - t_k)\right] = e^{F_x(\cdot)(t_{k+1}-t_k)} = \sum_{n=0}^{\infty} \frac{F_x^n(\cdot)(t_{k+1} - t_k)^n}{n!} \tag{17}$$

$$\Gamma_{k+1,k}(\cdot) = \exp\left[F_x(\cdot)(t_{k+1} - t_k)\right] \cdot F_u(\cdot) = \left(\sum_{n=0}^{\infty} \frac{F_x^n(\cdot)(t_{k+1} - t_k)^n}{n!}\right) \cdot F_u(\cdot) \tag{18}$$

Step 4: Covariance matrix of state prediction error

This step is based on the computation of the covariance matrix that corresponds to the error associated with the one-step ahead prediction that has been previously done based on the nonlinear models of the system. As it is possible to infer from the following equation, this covariance matrix depends on the covariance matrix of the process noise $\underline{\boldsymbol{w}}$, Q. This means that this matrix contains estimates of the uncertainty and correlation between uncertainties of state vector components.

$$P_{k+1,k}(\cdot) = \Phi_{k+1,k}(\cdot) P_{k,k}(\cdot) \Phi_{k+1,k}^T(\cdot) + \Gamma_{k+1,k}(\cdot) Q_{d,k}(\cdot) \Gamma_{k+1,k}^T(\cdot) \tag{19}$$

Step 5: Kalman gain calculation

As it will be possible to infer from Step 6, the Kalman gain acts as a weighting factor between current measurements and the state prediction. For the computation of this gain, the filter makes use of the available information about the uncertainties in the state estimates, using $P_{k+1,k}(\cdot)$; and in the measurements, using the covariance matrix of the measurement noise $\underline{\boldsymbol{v}}$, R.

$$K_{k+1}(\cdot) = P_{k+1,k}(\cdot) H_x^T(\cdot) \left[H_x(\cdot) P_{k+1,k}(\cdot) H_x^T(\cdot) + R_{k+1}\right]^{-1} \tag{20}$$

Step 6: Measurement update

Once the Kalman gain has been computed, it is now possible to proceed with the state estimation step by means of applying the weighted average between the measured and the predicted state, as presented in Eq. (21).

$$\underline{\hat{x}}_{k+1,k+1} = \underline{\hat{x}}_{k+1,k} + K_{k+1}(\cdot)\left[\underline{z}_{k+1} - \underline{h}\left(\underline{\hat{x}}_{k+1,k+1}, \underline{u}_{k+1}^*\right)\right] \tag{21}$$

Step 7: Covariance matrix of state estimation error

Finally, the value of the covariance matrix associated to the state estimation error needs to be computed in order to be used in the next iteration of the algorithm.

$$P_{k+1,k+1}\left(\cdot\right) = \left[I_n - K_{k+1}\left(\cdot\right) H_x\left(\cdot\right)\right] P_{k+1,k}\left(\cdot\right) \tag{22}$$

Once this point is reached, because of the recursiveness of the filter, the EKF starts again computing the one-step ahead prediction and all the aforementioned steps for the new t_{k+1} by means of using these results as the ones corresponding to t_k.

III.A.2. Analysis of state observability

Unlike its linear counterpart, the EKF is not an optimal estimator because of the nonlinearities of both the kinematic and observation models. In addition, if the initial estimate of the state is wrong, or if the process is modeled incorrectly, the filter may quickly diverge. However, in practice, and when used carefully, the Extended Kalman Filter can lead to a very reliable state estimation. This is particularly the case when the process being estimated can be accurately linearized at each point along the trajectory of the states and when the nonlinear mathematical model of the system is observable [20].

Based on this statement, and in order to make sure that the application of the Extended Kalman Filter is not going to diverge because of the proper definitions of the aircraft kinematic equations and observation model, the observability of the system is now assessed. By definition, the observability matrix for nonlinear systems is given by:

$$O = \begin{bmatrix} \partial_x h \\ \partial_x\left(L_f h\right) \\ \partial_x\left(L_f L_f h\right) \\ \vdots \\ \partial_x(\underbrace{L_f \ \ldots \ L_f}_{n-1} h) \end{bmatrix} \quad \text{with} \quad \begin{aligned} L_f h &= \partial_x h \cdot f \\ L_f L_f h &= \partial_x (L_f h) \cdot f \\ L_f L_f L_f h &= \partial_x (L_f L_f h) \cdot f \end{aligned} \tag{23}$$

The rank of this matrix for the nonlinear mathematical models introduced in Section II is equal to eighteen – the number of parameters in $\underline{\boldsymbol{x}}$, which means that the observability matrix for this nonlinear system is of full rank. This implies that the state vector can therefore be augmented in order to include sensor biases and wind components, and that it will not diverge because of this reason.

III.B. State Estimation Results

Once the Extended Kalman Filter has been introduced and the observability of the system has been demonstrated, now it is time to present the results obtained when the algorithm is applied in the state reconstruction of the Cessna Citation II when performing a set of maneuvers. For instance, one of the datasets analyzed corresponds to a 3211 maneuver in the ailerons, as presented in Figures (1) and (2).

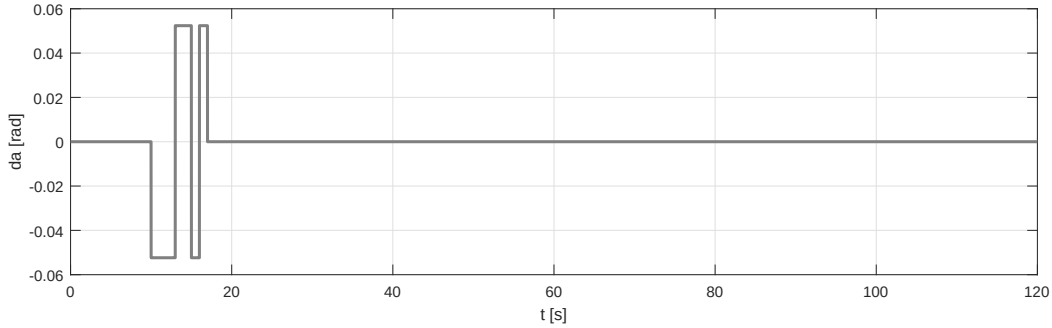

Figure 1: Control input in the ailerons for a 3211 maneuver

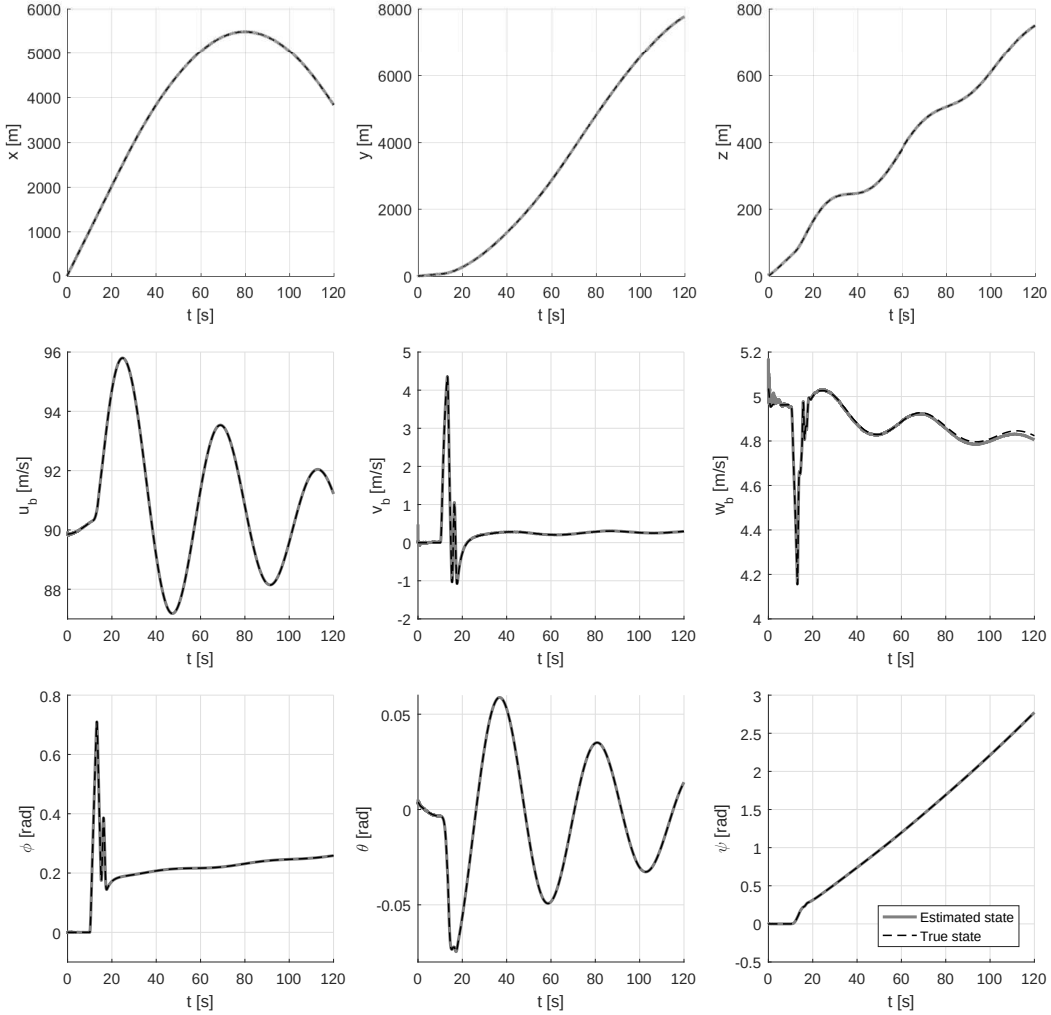

Figure 2: Aircraft state estimation for a 3211 maneuver in the ailerons

Once the main variables of the state vector have been reconstructed, it is also possible to compare the noise-dependent measurements and the same magnitudes, but in this case, computed using the state estimation as now presented.

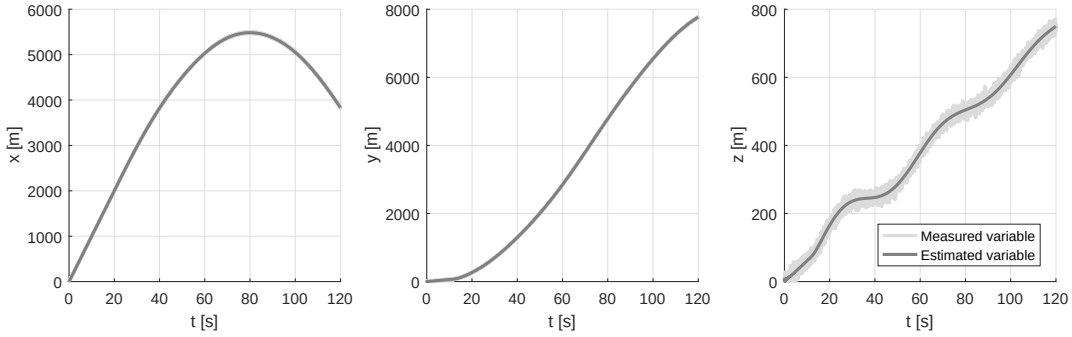

Figure 3: Aircraft magnitudes compared with on-board measurements for a 3211 maneuver in the ailerons

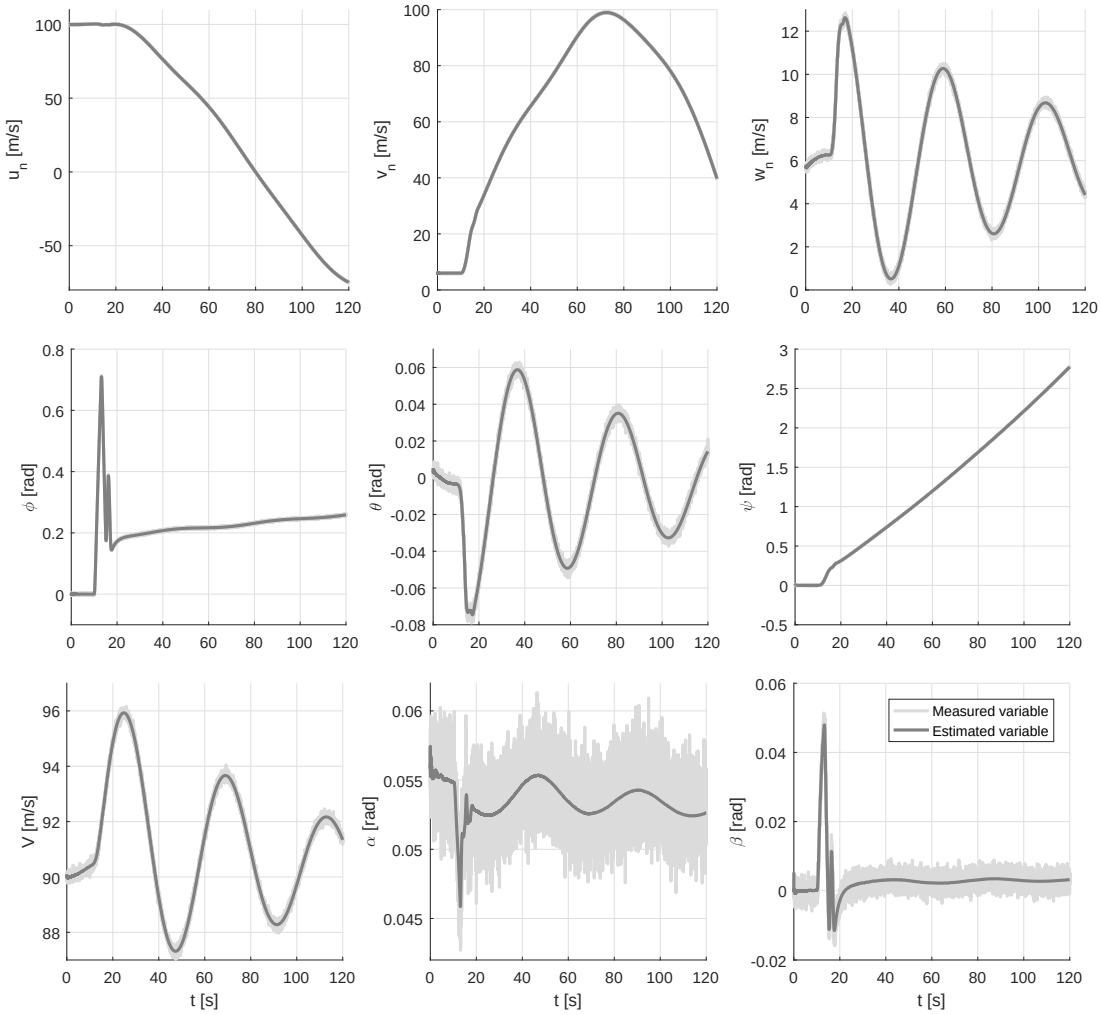

Figure 4: Aircraft magnitudes compared with on-board measurements for a 3211 maneuver in the ailerons

Regarding the set of unknown variables –sensor biases and wind components– that are part of the state vector as presented in Eq. (8), the utilization of the Extended Kalman Filter results in the following values for these parameters:

$$\left[\begin{array}{lll} \lambda_x = 8.4027 \cdot 10^{-4}\ m/s^2; & \lambda_p = 1.7522 \cdot 10^{-5}\ rad/s^2; & W_{x_n} = 10.0023\ m/s; \\ \lambda_y = 0.0018\ m/s^2; & \lambda_q = 1.8191 \cdot 10^{-5}\ rad/s^2; & W_{y_n} = 5.9990\ m/s; \\ \lambda_z = 1.6918 \cdot 10^{-4}\ m/s^2; & \lambda_r = 1.7559 \cdot 10^{-5}\ rad/s^2; & W_{z_n} = 0.9964\ m/s; \end{array}\right] \tag{24}$$

III.B.1. Analysis of convergence

Once these results are obtained, it is of relevant importance to analyze the accuracy of the state estimation performed by the Kalman filter. In order to do so, these results are compared with a set of reference signals in order to compute the error during the estimation of the state vector. Finally, the convergence of the results is ensured by means of studying how this error evolves with respect to its standard deviation, parameter known as *Innovation*.

As it is possible to infer from Figure 5, it is of relevant importance to mention the high accuracy of the state estimation that the Kalman filter has performed by means of combining the available measurements coming from the GPS/IMU/Airdata navigation system and its own predictions. This accuracy is ensured when the estimated error converges into a value inside the innovation. Based on this statement, there are two particular plots in this figure that need to be individually assessed: the error in the estimation of the x position and of the velocity w_b.

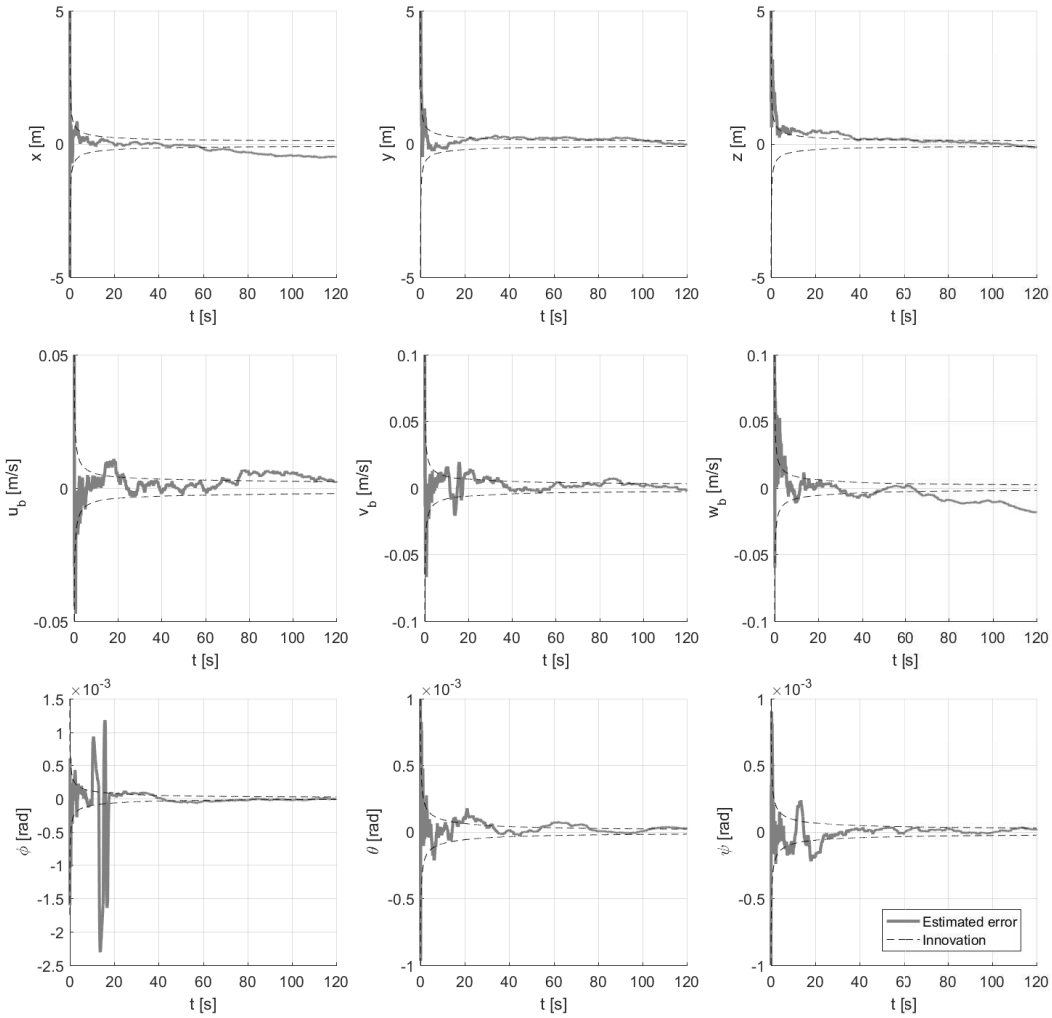

Figure 5: Proof of convergence. Estimated error and innovation for a 3211 maneuver in the ailerons

Firstly, the estimated error for the position in the x axis does not converge into the region determined by its innovation. However, as it is possible to observe in the figure, it presents a convergence tendency towards a value just a bit biased from where it should be. Furthermore, this bias can be considered negligible when compared to the order of magnitude of x. Therefore, the estimation obtained for this parameter should not be treated as an important source of error for the incoming parameter estimation step of the Two-Step Approach.

Secondly, the estimated error for the velocity in the z axis of the body-fixed reference frame, w_b, presents a divergence behaviour in the second half of the maneuver that is being analyzed. These divergence properties imply that this will be a considerable error source during the estimation of the aerodynamic model of the aircraft, so it is important to take this parameter into account in order to determine statistical quality of the parameter estimates that are about to be computed.

Once this analysis is completed, it is also relevant to present the proof of convergence of the set of unknown variables that augmented the state vector, as mentioned above. These results are presented in Figure 6. In this case, it is important to remark that both the estimated error for λ_y and for λ_z present certain biases with respect to the region determined by their innovation. As in the case of w_b, because of the order of magnitude of the biases, these inaccuracies may have an effect in the quality of the results of the following steps.

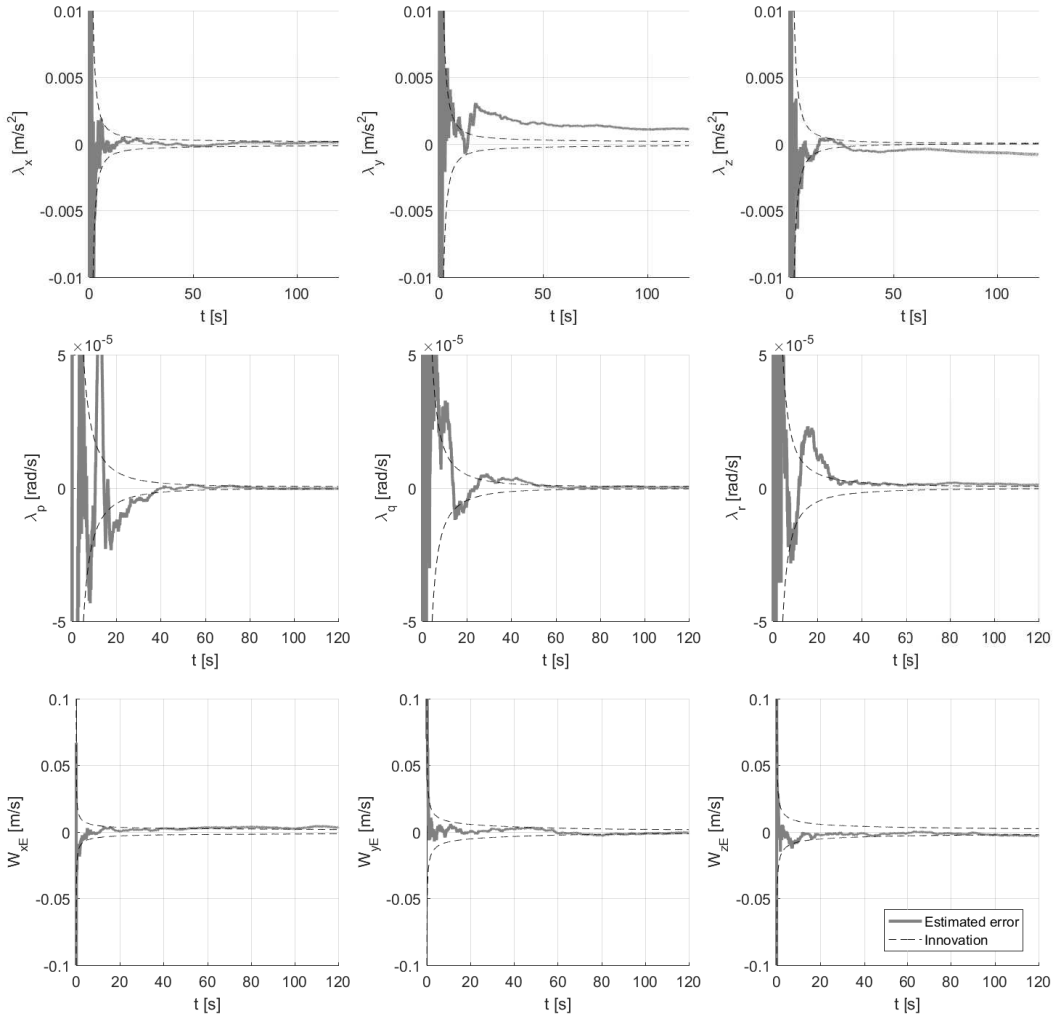

Figure 6: Proof of convergence. Estimated error and innovation for a 3211 maneuver in the ailerons

IV. Aerodynamic Model Identification

The second step of the Two-Step Identification Approach consists in the estimation of the dimensionless coefficients which comprise the aerodynamic model of the Cessna Citation II. In order to do so, simple regression methods can be applied to estimate these coefficients because the aerodynamic model becomes linear-in-the-parameters with respect to the magnitudes obtained from the flight path reconstruction problem.

This section presents the theory behind the implementation of the Ordinary Least Squares (OLS) algorithm as the regression method selected; the aerodynamic model estimated for this aircraft; and a proof of the statistical quality of the results.

IV.A. Aerodynamic forces and moments

Before starting with the estimation and identification tasks that are involved in this second part of the Two-Step Approach, it is of relevant importance to understand what is an aerodynamic model in itself. The aerodynamic model of an aircraft is a set of coefficients –also known as aerodynamic coefficients– that are used for the computation of the dimensionless counterparts of the aerodynamic forces and moments that characterize that aircraft in particular. When the aerodynamic model of an aircraft is known, it is possible to use this knowledge in a variety of applications, such as the creation of adaptive control systems or the development of dynamic models for flight simulators.

Based on this explanation, the first step in the identification of the aerodynamic model of the Cessna Citation II consists in the utilization of the results previously obtained in order to compute the expressions for the dimensionless aerodynamic forces and moments, as now presented. Eq. (25) corresponds to the set of aerodynamic forces, and Eq. (26) to the aerodynamic moments.

$$\begin{aligned} C_X &= \frac{X}{\frac{1}{2}\rho V^2 S} = \frac{mA_x}{\frac{1}{2}\rho V^2 S}; \\ C_Y &= \frac{Y}{\frac{1}{2}\rho V^2 S} = \frac{mA_y}{\frac{1}{2}\rho V^2 S}; \\ C_Z &= \frac{Z}{\frac{1}{2}\rho V^2 S} = \frac{mA_z}{\frac{1}{2}\rho V^2 S}; \end{aligned} \tag{25}$$

$$\begin{aligned} C_l &= \frac{L}{\frac{1}{2}\rho V^2 Sb} = \frac{\dot{p}I_{xx}+qr(I_{zz}-I_{yy})-(pq+\dot{r})I_{xz}}{\frac{1}{2}\rho V^2 Sb}; \\ C_m &= \frac{M}{\frac{1}{2}\rho V^2 S\overline{c}} = \frac{\dot{q}I_{yy}+rp(I_{xx}-I_{zz})-(p^2-r^2)I_{xz}}{\frac{1}{2}\rho V^2 S\overline{c}}; \\ C_n &= \frac{N}{\frac{1}{2}\rho V^2 Sb} = \frac{\dot{r}I_{zz}+pq(I_{yy}-I_{xx})-(qr-\dot{p})I_{xz}}{\frac{1}{2}\rho V^2 Sb}; \end{aligned} \tag{26}$$

Based on [22] and before any computation, it is important to remark that this set of coefficients can also be grouped in terms of the aircraft dynamics –longitudinal or lateral– to which they pertain. On one hand, C_X, C_Z, and C_m are the coefficients associated with the longitudinal dynamics. The reason for this relies on the fact that these terms are different from zero if and only if the elevator is used during the maneuver. On the other hand, the coefficients C_Y, C_l, and C_n are associated with the aircraft lateral dynamics because they are non-zero when the rudder or the ailerons are employed. Because of this reason, it is also important to classify the datasets provided in this assignment as longitudinal or lateral databases.

The results previously presented in this report as part of the flight path reconstruction problem corresponded to the dataset `da3211`, which is a 3211 maneuver in the ailerons. Therefore, it can be labeled as a lateral dataset. Apart from this maneuver, the datasets `dadoublet`, `dr3211`, and `drdoublet` are also part of this group, and therefore, their data will only be used in the computation of the lateral aerodynamic coefficients. On the other hand, the set `de3211`, which corresponds to a 3211 maneuver in the elevator, corresponds to the only dataset labeled as longitudinal.

Once this has been clarified, the sets of coefficients presented in Eqs. (25) and (26) are computed with the aid of Eq. (5) in order to obtain the unbiased version of the linear accelerations –A_x, A_y, and A_z– and angular velocities –p, q and r–. Additionally, numerical differentiation has been applied for the obtaining of the set of angular accelerations –$\dot{p}, \dot{q}$ and $\dot{r}$–, and other data of the aircraft is listed as follows.

$$I_{xx} = 11,187.8\ kg\ m^2; \quad I_{yy} = 22,854.8\ kg\ m^2; \quad I_{zz} = 31,974.8\ kg\ m^2; \quad I_{xz} = 1,930.1\ kg\ m^2;$$
$$\text{mass} : 4,500\ kg; \quad \text{wing span} : b = 13.3250\ m; \quad \text{wing area} : S = 24.9900\ m^2; \quad \text{chord} : \overline{c} = 1.9910;$$

IV.B. Least squares parameter estimator

The aerodynamic forces and moment coefficients introduced in Eqs. (25) and (26) can be expressed in terms of several state and control variables of the vehicle, as now presented:

$$\begin{Bmatrix} C_X \\ C_Z \\ C_m \end{Bmatrix} = f(\alpha, \alpha^2, q, \delta_e); \quad \begin{Bmatrix} C_Y \\ C_l \\ C_n \end{Bmatrix} = f(\beta, p, r, \delta_a, \delta_r); \tag{27}$$

Moreover, each coefficient in Eq. (27) can be expressed in a Taylor series expansion as a function of the state and control variables. If terms up to the first order are included in this expansion, these coefficients are expressed as follows:

$$\begin{aligned} C_X &= C_{X_0} + C_{X_\alpha}\alpha + C_{X_{\alpha^2}}\alpha^2 + C_{X_q}\frac{q\overline{c}}{V} + C_{X_{\delta_e}}\delta_e; \\ C_Z &= C_{Z_0} + C_{Z_\alpha}\alpha + C_{Z_q}\frac{q\overline{c}}{V} + C_{Z_{\delta_e}}\delta_e; \\ C_m &= C_{m_0} + C_{m_\alpha}\alpha + C_{m_q}\frac{q\overline{c}}{V} + C_{m_{\delta_e}}\delta_e; \end{aligned} \tag{28}$$

$$
\begin{aligned}
C_Y &= C_{Y_0} + C_{Y_\beta}\beta + C_{Y_p}\frac{pb}{2V} + C_{Y_r}\frac{rb}{2V} + C_{Y_{\delta_a}}\delta_a + C_{Y_{\delta_r}}\delta_r; \\
C_l &= C_{l_0} + C_{l_\beta}\beta + C_{l_p}\frac{pb}{2V} + C_{l_r}\frac{rb}{2V} + C_{l_{\delta_a}}\delta_a + C_{l_{\delta_r}}\delta_r; \\
C_n &= C_{n_0} + C_{n_\beta}\beta + C_{n_p}\frac{pb}{2V} + C_{n_r}\frac{rb}{2V} + C_{n_{\delta_a}}\delta_a + C_{n_{\delta_r}}\delta_r;
\end{aligned} \tag{29}
$$

where each coefficient in Eqs. (28) and (29) expresses the effect of its corresponding parameter on the total aerodynamic forces and moments. Therefore, these are the coefficients that need to be estimated in this second step of the Two-Step Identification Approach. Note that this analysis does not include the effect that thrust parameters may have along the X and Z axes, nor the pitching moment around the Y axis that they may induce.

Based on this notation, each of the aerodynamic forces and moment coefficients can be expressed as presented in Eq. (30).

$$
y(i) = \theta_0 + \theta_1 x_1(i) + \theta_2 x_2(i) + \ \ldots \ + \theta_p x_p(i) + \epsilon(i); \qquad \text{with } i = 1, 2, ..., N; \tag{30}
$$

where $y(i)$ is the dependent variable – the aerodynamic forces and moment coefficients–, $x_p(i)$ denote the independent variables –the estimated state and control variables–, θ_p is the vector of the aerodynamic parameters, and $\epsilon(i)$ is the stochastic equation error, accounting for measurement as well as model errors on the dependent variable. Finally, N denotes the number of data that corresponds to that specific dependent variable.

Eq. (30) can also be written in matrix form as introduced in Eq. (31), where $A(x)$ is denoted as the regression matrix.

$$
\boldsymbol{y} = \boldsymbol{A}(\boldsymbol{x}) \cdot \boldsymbol{\theta} + \boldsymbol{\epsilon} \quad \rightarrow \quad \begin{Bmatrix} y(1) \\ y(2) \\ \ldots \\ y(N) \end{Bmatrix} = \begin{bmatrix} 1 & x_{12} & \ldots & x_{1p} \\ 1 & x_{22} & \ldots & x_{2p} \\ \ldots & \ldots & \ldots & \ldots \\ 1 & x_{N2} & \ldots & x_{Np} \end{bmatrix} \begin{Bmatrix} \theta_1 \\ \theta_2 \\ \ldots \\ \theta_p \end{Bmatrix} + \begin{Bmatrix} \epsilon_1 \\ \epsilon_2 \\ \ldots \\ \epsilon_p \end{Bmatrix} \tag{31}
$$

Once the identification problem is formulated using this notation, it is now possible to proceed with the implementation of the Ordinary Least Squares (OLS) algorithm. This technique, by definition [23], provides an estimate of the parameters that is the one that yields the least (or minimum) sum of squared residuals. Based on this statement, the cost function is defined as follows:

$$
J(\boldsymbol{\theta}) = \boldsymbol{\epsilon}^T \boldsymbol{\epsilon} = (\boldsymbol{y} - \boldsymbol{A}(\boldsymbol{x}) \cdot \boldsymbol{\theta})^T (\boldsymbol{y} - \boldsymbol{A}(\boldsymbol{x}) \cdot \boldsymbol{\theta}) \tag{32}
$$

and the estimated solution that minimizes this cost function is given by:

$$
\hat{\boldsymbol{\theta}} = (\boldsymbol{A}(\boldsymbol{x})^T \boldsymbol{A}(\boldsymbol{x}))^{-1} \boldsymbol{A}(\boldsymbol{x})^T \boldsymbol{y} \tag{33}
$$

Following the estimated parameter $\hat{\boldsymbol{\theta}}$, the estimated dependent variable, $\hat{\boldsymbol{y}}$, and the estimated error model (residual), $\hat{\boldsymbol{\epsilon}}$, can be calculated from:

$$
\hat{\boldsymbol{y}} = \boldsymbol{A}(\boldsymbol{x}) \cdot \hat{\boldsymbol{\theta}}; \qquad\qquad \hat{\boldsymbol{\epsilon}} = \boldsymbol{y} - \hat{\boldsymbol{y}} = \boldsymbol{y} - \boldsymbol{A}(\boldsymbol{x}) \cdot \hat{\boldsymbol{\theta}}; \tag{34}
$$

Implementing this technique, it is possible to compute the estimated parameter vector, $\hat{\boldsymbol{\theta}}$, and the residual vector, $\hat{\boldsymbol{\epsilon}}$, for each of the six different aerodynamic forces and moment coefficients presented in Eqs. (28) and (30). These results are presented in the following subsection.

IV.C. Estimated aerodynamic model

The results obtained by means of applying Eq. (33) to each of the aerodynamic forces and moment coefficients –each one with its own set variables– are now presented in Tables 1 and 2.

	C_{i_0}	C_{i_α}	$C_{i_{\alpha 2}}$	$C_{i_{\bar{q}}}$	$C_{i_{\delta_e}}$
$i = X$	-0.0143	0.0985	3.0472	-1.4209	-0.0231
$i = Z$	-0.1237	-4.4927		-5.4033	-0.4192
$i = m$	0.0189	-0.5883		0.6483	-0.5582

Table 1: Estimated aerodynamic coefficients - Longitudinal dynamics

	C_{i_0}	C_{i_β}	$C_{i_{\bar{p}}}$	$C_{i_{\bar{r}}}$	$C_{i_{\delta_a}}$	$C_{i_{\delta_r}}$
$i = Y$	-0.0001	-0.4617	-0.1061	0.7190	-0.0445	0.0607
$i = l$	-2.571e-05	-0.0513	-0.1342	0.1399	-0.0748	0.0093
$i = n$	1.643e-05	0.0354	-0.0561	-0.0949	-0.0231	-0.0207

Table 2: Estimated aerodynamic coefficients - Lateral dynamics

Using these parameters, it is possible to estimate the dependent variables $\hat{\boldsymbol{y}}$ for each of these coefficients and compare them with the original values for $\{C_X, C_Y, C_Z, C_l, C_m, C_n\}$ that were computed using extended Kalman filter results. Subsequently, the aforementioned residuals become available for analysis.

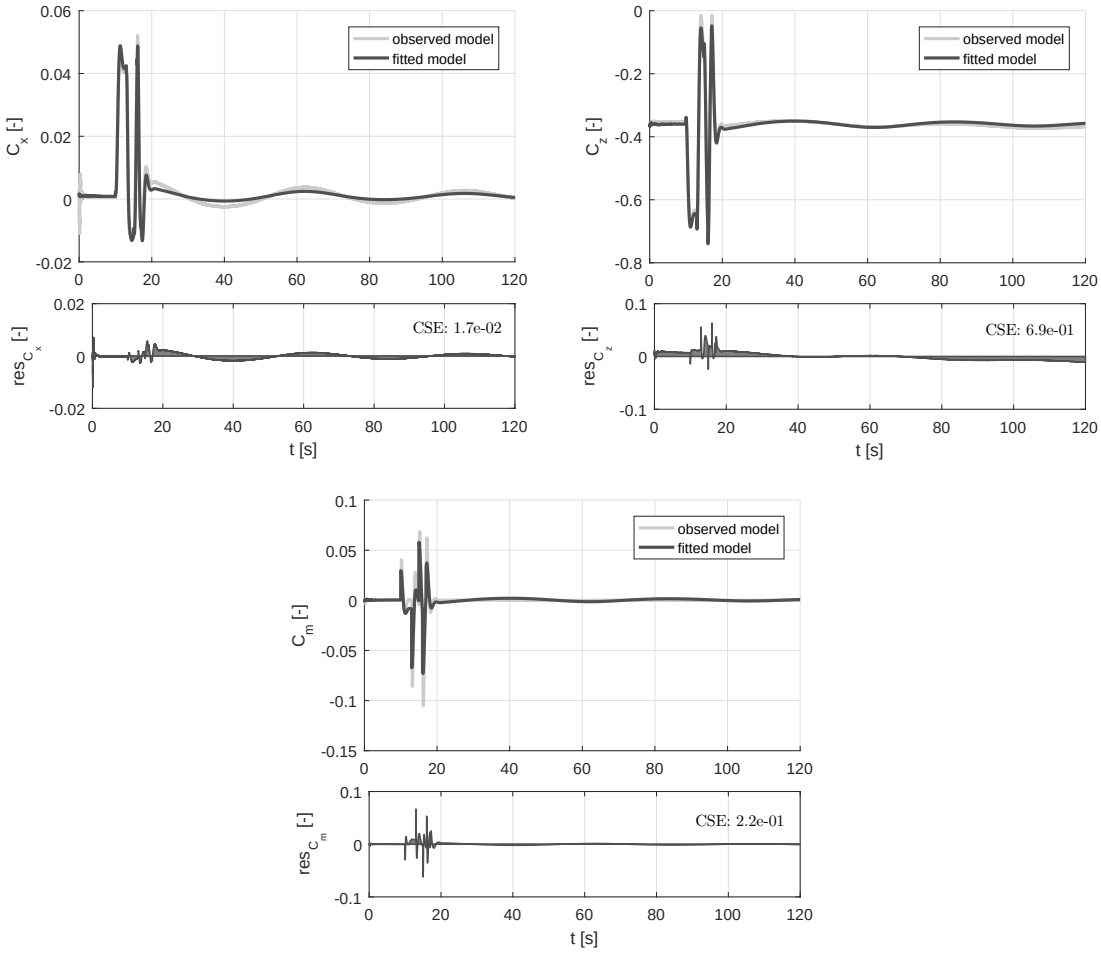

Figure 7: Aerodynamic model validation - Longitudinal dynamics

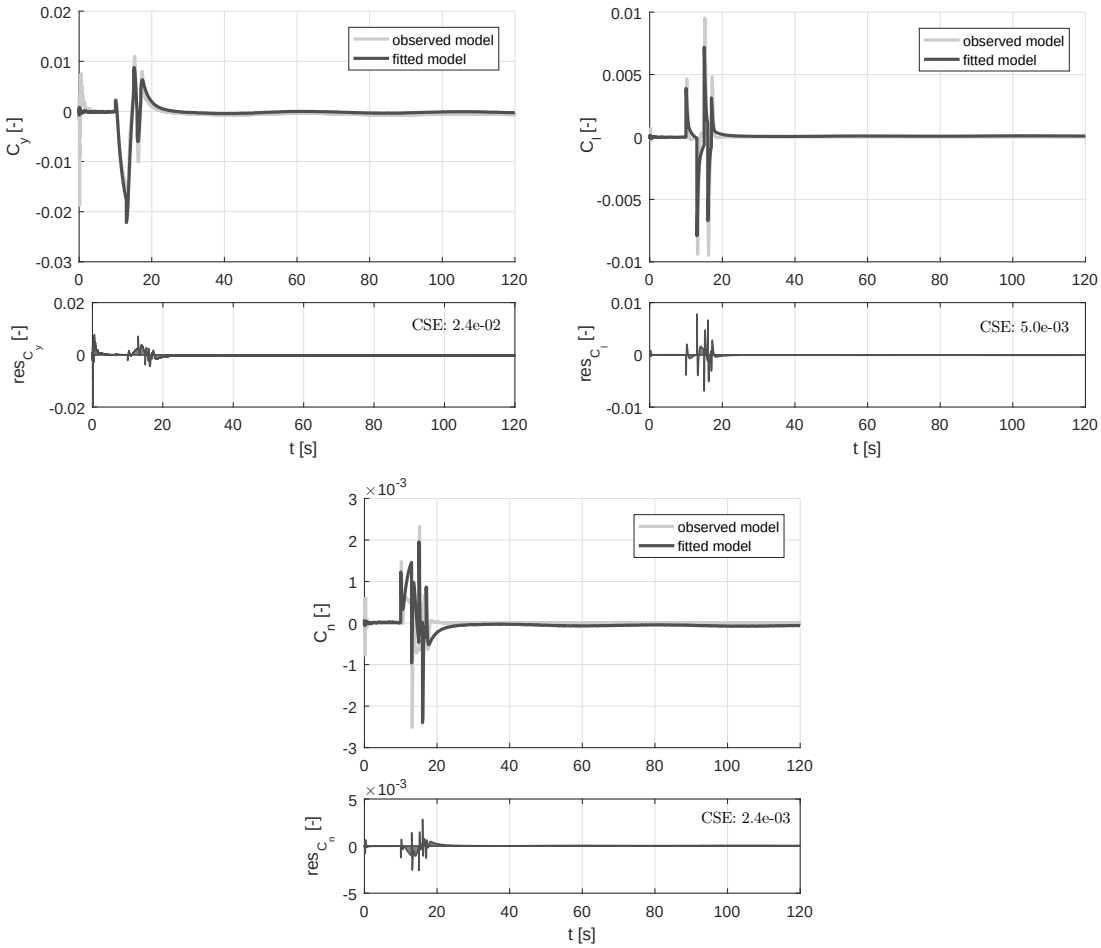

Figure 8: Aerodynamic model validation - Lateral dynamics

As it is possible to observe from Figures 7 and 8, the estimations for the aerodynamic coefficients that have been obtained with the OLS algorithm present a remarkable accuracy when compared with the original values of these parameters. This means that the regression method selected (OLS) has been able to fit the data provided for each of these coefficients in such an accurate way that, when the coefficients are re-computed using Eqs. (28) and (29), there is a considerable similarity between the original and the estimated parameters.

This statement is reinforced by means of analyzing what has been denominated as the "'Cumulative Squared Error"' (CSE) introduced in Eq. (35). Because the OLS algorithm is a regression method that fits the data via the minimization of the sum of squared errors, this analysis uses the cumulative sum of these squared errors in order to assess the quality of the results.

$$CSE = \sum_{i=1}^{N} \left(\boldsymbol{y}(i) - \hat{\boldsymbol{y}}(i) \right)^2 ; \tag{35}$$

Based on the definition of this parameter, which is included in all the plots from Figures 7 and 8, it is important to remark that the estimation obtained for C_Z –and its associated coefficients– is the less accurate, as its CSE is of the order of 10^{-1}. Taking also into account the divergence properties of the EKF estimation for the velocity w_b, which is directly related with the aerodynamic force in this axis, it is possible to say that the set of parameter comprised by $\left\{ C_{Z_0}, C_{Z_\alpha}, C_{Z_{\bar{q}}}, C_{Z_{\delta_e}} \right\}$ is the less accurate when compared with the real values of these coefficients. On the other hand, because of the CSE values obtained for C_l and C_n, the sets of aerodynamic coefficients related to these parameters are probably the most accurate when compared with the real-life values of this aircraft.

Another analysis which is of relevant importance when studying these results consists in the fact of detecting which model terms are most dominant and which have the least influence during the execution of the regression method selected. In order to detect these terms, it is important to state that the overall effect of one of these aerodynamic coefficients in the data fitting depends on the order of magnitude of the product between the estimated parameter and the maximum value of the corresponding independent variable $x_p(i)$. These results are presented in Tables 3 and 4.

	C_{i_0}	$C_{i_\alpha} \cdot \max(\alpha)$	$C_{i_{\alpha^2}} \cdot \max(\alpha^2)$	$C_{i_{\bar{q}}} \cdot \max(\bar{q})$	$C_{i_{\delta_e}} \cdot \max(\delta_e)$
$i = X$	-0.0143	0.0129	0.0533	-0.0061	-0.0007
$i = Z$	-0.1236	-0.5932		-0.0226	-0.0115
$i = m$	0.0189	-0.0777		0.0028	-0.0154

Table 3: Aerodynamic coefficients influence in data fitting - Longitudinal dynamics

	C_{i_0}	$C_{i_\beta} \cdot \max(\beta)$	$C_{i_{\bar{p}}} \cdot \max(\bar{p})$	$C_{i_{\bar{r}}} \cdot \max(\bar{r})$	$C_{i_{\delta_a}} \cdot \max(\delta_a)$	$C_{i_{\delta_r}} \cdot \max(\delta_r)$
$i = Y$	-0.0001	-0.0222	-0.0022	0.0042	-0.0023	0.0032
$i = l$	-2.571e-05	-0.0025	-0.0028	0.0008	-0.0039	0.0005
$i = n$	1.643e-05	0.0017	-0.0012	-0.0005	-0.0012	-0.0011

Table 4: Aerodynamic coefficients influence in data fitting - Lateral dynamics

Based on these results, it is possible to infer that the model terms with a higher influence in the data fitting correspond to the angle-of-attack, α, for the aircraft longitudinal dynamics; and to the sideslip angle, β, for the lateral case. On the other hand, the dimensionless representations of the angular rates, $\{\bar{p},\ \bar{q},\ \bar{r}\}$, are the model terms with the lowest influence in this identification task. This is a beneficial conclusion in terms of the accuracy of the results. The reason for this is that these parameters, α and β, were reconstructed accurately using the extended Kalman filter as presented in previous sections of these report. However, the aircraft angular rates were noise-affected biased signals that were approximately corrected from these biases with the results obtained in the EKF, but whose noisy components are still present in the signals.

Finally, the last step in the validation of these results consists in the utilization of an alternative model structure in this aerodynamic identification step in order to see if this improves the accuracy of the results. In order to proceed, the aerodynamic model presented in Eqs. (28) and (29) is augmented by means of adding the pitch angle in the longitudinal model, and the roll and yaw angles in the lateral model. This alternative structure is introduced in Eqs. (36) and (37).

$$\begin{aligned} C_X &= C_{X_0} + C_{X_\alpha}\alpha + C_{X_{\alpha^2}}\alpha^2 + C_{X_\theta}\theta + C_{X_q}\frac{q\bar{c}}{V} + C_{X_{\delta_e}}\delta_e; \\ C_Z &= C_{Z_0} + C_{Z_\alpha}\alpha + C_{Z_\theta}\theta + C_{Z_q}\frac{q\bar{c}}{V} + C_{Z_{\delta_e}}\delta_e; \\ C_m &= C_{m_0} + C_{m_\alpha}\alpha + C_{m_\theta}\theta + C_{m_q}\frac{q\bar{c}}{V} + C_{m_{\delta_e}}\delta_e; \end{aligned} \tag{36}$$

$$\begin{aligned} C_Y &= C_{Y_0} + C_{Y_\beta}\beta + C_{Y_\phi}\phi + C_{Y_\psi}\psi + C_{Y_p}\frac{pb}{2V} + C_{Y_r}\frac{rb}{2V} + C_{Y_{\delta_a}}\delta_a + C_{Y_{\delta_r}}\delta_r; \\ C_l &= C_{l_0} + C_{l_\beta}\beta + C_{l_\phi}\phi + C_{l_\psi}\psi + C_{l_p}\frac{pb}{2V} + C_{l_r}\frac{rb}{2V} + C_{l_{\delta_a}}\delta_a + C_{l_{\delta_r}}\delta_r; \\ C_n &= C_{n_0} + C_{n_\beta}\beta + C_{n_\phi}\phi + C_{n_\psi}\psi + C_{n_p}\frac{pb}{2V} + C_{n_r}\frac{rb}{2V} + C_{n_{\delta_a}}\delta_a + C_{n_{\delta_r}}\delta_r; \end{aligned} \tag{37}$$

As done before, the results obtained by means of applying Eq. (33) to each of the aerodynamic forces and moment coefficients are now presented in Tables 5 and 6.

	C_{i_0}	C_{i_α}	$C_{i_{\alpha^2}}$	C_{i_θ}	$C_{i_{\bar{q}}}$	$C_{i_{\delta_e}}$
$i = X$	-0.0143	0.0976	3.0694	-0.0003	-1.4352	-0.0233
$i = Z$	-0.1223	-4.5227		0.0116	-4.9938	-0.4169
$i = m$	0.0198	-0.6070		0.0089	0.8411	-0.5585

Table 5: Estimated aerodynamic coefficients (alternative model) - Longitudinal dynamics

	C_{i_0}	C_{i_β}	C_{i_ϕ}	C_{i_ψ}	$C_{i_{\bar{p}}}$	$C_{i_{\bar{r}}}$	$C_{i_{\delta_a}}$	$C_{i_{\delta_r}}$
$i = Y$	-0.0001	-0.4738	-0.0093	-0.0004	0.0127	2.0988	-0.0188	0.1171
$i = l$	-1.966e-08	-0.0514	-0.0046	-2.747e-05	-0.0318	0.7010	-0.0635	0.0093
$i = n$	1.292e-05	0.0406	-2.446e-04	1.258e-04	-0.0583	-0.1613	-0.0232	-0.0240

Table 6: Estimated aerodynamic coefficients (alternative model) - Lateral dynamics

This set of results is now used to compute the CSE –introduced in Eq. (35)– for each of these coefficients in order to determine if the fact of modifying the aerodynamic model has been useful for a better estimation using the Ordinary Least Squares regression method. Table 7 presents the CSE values for both the original and the modified aerodynamic models, and indeed, it is possible to infer that the fact of augmenting the model has no impact in the accuracy of the results.

	C_X	C_Z	C_m	C_Y	C_l	C_n
CSE_{org}	1.7e-02	6.9e-01	2.2e-01	2.4e-02	5.0e-03	2.4e-03
CSE_{mod}	1.8e-02	6.8e-01	2.2e-01	1.6e-02	4.1e-03	2.3e-03

Table 7: Estimated aerodynamic coefficients (alternative model) - Longitudinal dynamics

V. Conclusions

The main goal of this practical assignment is to familiarize with the processes and methodologies typically conducted in the identification of the aerodynamic model of an aircraft from raw flight-test data using the Two-Step Identification Method. This goal has been pursued by conducting the implementation of the extended Kalman filter (EKF) and by using the Ordinary Least Squares (OLS) regression method. From the study carried out, a number of relevant conclusions can be drawn.

In this report, the extended Kalman filter is presented as a viable algorithm to perform the task of flight path reconstruction with a promising level of accuracy in its results. As discussed in Section III, the EKF state vector can be augmented in order to estimate sensor biases and wind components without implying the divergence of its results. Furthermore, in this section it is also possible to observe how all the unknown states converge to their real values with the exception of some parameters as w_b or λ_y.

Finally, Section IV presents the implementation of the OLS algorithm in order to fit the EKF data into a previously specified aerodynamic model structure. This section also contains the validation of this task, confirming that indeed, the desired aerodynamic coefficients are estimated accurately. Moreover, the fact that α and β are the dominant terms of this model is also demonstrated during this validation. Finally, this section contains the proof that augmenting the aerodynamic model to cover extra parameters –such as $\{\phi, \theta, \psi\}$– does not imply a better accuracy in this identification step.

References

[1]Braga de Mendonça, C., Moreira Hemerly, E., and Sandoval Góes, L.C. *Adaptive Stochastic Filtering for Online Aircraft Flight Path Reconstruction.* Journal of Aircraft, Vol. 44, No. 5, September-October 2007.

[2]Sieberling, S., Chu, Q.P., and Mulder, J.A. *Robust Flight Control Using Incremental Nonlinear Dynamic Inversion and Angular Acceleration Prediction.* Journal of Guidance, Control, and Dynamics, Vol. 33, No. 6, November-December 2010.

[3]Norton, W.J. *Balancing Modeling and Simulation with Flight test in Military Aircraft Development.* AGARD CP-593, December 1997.

[4]Jategaonkar, R., Fischenberg, D., and von Gruenhagen, W. *Aerodynamic Modeling and System Identification from Flight Data - Recent Applications at DLR.* Journal of Aircraft, Vol. 41, July-August 2004.

[5]Jonkers, H.L. *Application of the Kalman Filter to Flight Path Reconstruction from Flight Test Data Including Estimation of Instrumental Bias Error Corrections.* Department of Aerospace Engineering, Rept. VTH-162, 1976.

[6]Klein, V., and Schiess, J.R. *Compatibility Check of Measured Aircraft Responses Using Kinematic Equations and Extended Kalman Filter.* NASA TN D-8514, August 1977.

[7]Teixeira, B.O.S., Torres, L.A.B., Iscold, P., and Aguirre, L.A. *Flight path reconstruction - A comparison of nonlinear Kalman filter and smoother algorithms.* Aerospace Science and Technology, August 2010.

[8]Grauer, J.A. *Real-Time Parameter Estimation Using Output Error.* NASA Langley Research Center.

[9]Mulder, J.A., Chu, Q.P., Sridhar, J.K., Breeman, J.H., and Laban, M. *Non-linear aircraft flight path reconstruction review and new advances.* Progress in Aerospace Sciences, Vol. 35, No. 7, October 1999.

[10]Teixeira, B.O.S., Torres, L.A.B., Iscold, P., and Aguirre, L.A. *Flight Path Reconstruction using the Unscented Kalman Filter Algorithm.* 18th International Congress of Mechanical Engineering, November 2005.

[11]Girich, C., and Ravindra, J. *Aerodynamic Parameter Estimation from Flight Data Applying Extended and Unscented Kalman Filter.* Journal of Aerospace Science and Technology, Vol. 14, No. 2, 2010.

[12]Chu, Q.P., Mulder, J.A., and van Woerkom, P.T.L.M. *Modified Recursive Maximum Likelihood Adaptive Filter for Nonlinear Aircraft Flight-Path Reconstruction.* Journal of Guidance, Control, and Dynamics, November-December 1996.

[13]Babuska, R. *Knowledge-Based Control Systems, Lecture Notes.* Delft University of Technology, January 2010.

[14]Ferrari, S., and Stengel, R.F. *Smooth function approximation using neural networks.* IEEE Transactions On Neural Networks, Januray 2005.

[15]Akpan, V.A., and Hassapis, G.D. *Nonlinear model identification and adaptive model predictive control using neural networks.* ISA Transactions, Vol. 50, No. 2, April 2011.

[16]de Visser, C.C. *Global Nonlinear Model Identification with Multivariate Splines.* Published PhD thesis, Delft University of Technology, 2011.

[17]de Visser, C.C., and Mulder, J.A. *Global Nonlinear Aerodynamic Model Identification with Multivariate Splines.* AIAA Atmospheric Flight Mechanics Conference, August 2009.

[18]Visser, T., de Visser, C.C., and van Kampen, E. *Quadrotor System Identification using the Multivariate Multiplex B-Spline.* AIAA Atmospheric Flight Mechanics Conference, January 2015.

[19]Etkin, B. *Dynamics of atmospheric flight.* Wiley, 1972.

[20]Groves, P.D. *Principles of GNSS, Inertial, and Multisensor Integrated Navigation Systems.* Artech House, 2008.

[21]de Visser, C., Pool, D., and van Kampen, E. *System Identification of Aerospace Vehicles, Lecture Notes.* Delft University of Technology, April 2016.

[22]Roskam, J. *Airplane Flight Dynamics and Automatic Flight Controls, Part I.* Design, Analysis and Research Corporation, 2001.

[23]Puntanen, S., and Styan, G.P.H. *The Equality of the Ordinary Least Squares Estimator and the Best Linear Unbiased Estimator.* The American Statician, Val. 43, 1989.